water

MDPI

Article

Enhancing Groundwater Resource Management in the Milan Urban Area Through a Robust Stratigraphic Framework and Numerical Modeling

Luca Alberti [1], Pietro Mazzon [1,*], Loris Colombo [1], Martino Cantone [1], Matteo Antelmi [1,*], Fabio Marelli [2] and Paola Gattinoni [1]

[1] Environmental and Civil Engineering Department, Politecnico di Milano, 20133 Milan, Italy; luca.alberti@polimi.it (L.A.); loris.colombo@polimi.it (L.C.); martino.cantone@polimi.it (M.C.); paola.gattinoni@polimi.it (P.G.)
[2] MM Spa, 20121 Milan, Italy; f.marelli@mmspa.eu
* Correspondence: pietro.mazzon@polimi.it (P.M.); matteo.antelmi@polimi.it (M.A.)

Abstract: Groundwater is a critical freshwater resource in Italy's Po plain, which includes Milan (northern Italy), one of Europe's most industrialized and urbanized areas. This region relies heavily on groundwater for both industrial and public water supplies. However, the quantity and quality of this resource are vulnerable to both natural and human-induced factors, such as climate change, industrial activities, and changing water use practices. This study investigates and addresses the complex management challenges of groundwater resources of Milan in the framework of the EU directives. A steady-state groundwater flow model was developed as part of the broader project MODEL-MI to aid in the creation of a Water Safety Plan (WSP). This study highlights the importance of accurate stratigraphic data to constructing a reliable hydrogeological conceptual model. The model, calibrated using extensive data, successfully reproduces groundwater flow patterns and will be used both to support decision-making for sustainable groundwater management and to predict future impacts of climate change on water resources.

Keywords: groundwater; numerical modeling; hydrostratigraphy; Milan urban area; water management; water safety plan

Academic Editor: Adriana Bruggeman

Received: 31 October 2024
Revised: 25 December 2024
Accepted: 30 December 2024
Published: 9 January 2025

Citation: Alberti, L.; Mazzon, P.; Colombo, L.; Cantone, M.; Antelmi, M.; Marelli, F.; Gattinoni, P. Enhancing Groundwater Resource Management in the Milan Urban Area Through a Robust Stratigraphic Framework and Numerical Modeling. *Water* **2025**, *17*, 165. https://doi.org/10.3390/w17020165

1. Introduction

Groundwater is the largest body of freshwater in the world and the main source of public drinking water supplies in many European regions. This is also the case of the Po plain area in Lombardy (northern Italy), which includes the metropolitan area of Milan, which is one of the most relevant urbanized and industrial areas in Europe.

In urban areas, both natural causes (e.g., climate change) and human-induced processes (e.g., changing in withdrawal and/or irrigation practices) can affect groundwater availability [1–5]. Furthermore, the presence of possible sources of groundwater pollution is a matter of concern when dealing with water availability in terms of quality [6,7]. Moreover, the influence of GWHP systems on aquifers underneath cities has been demonstrated by several authors [8–13] who found out that in several aquifers in European cities, abnormal effects in the aquifer's temperature were probably caused by intensive use of the geothermal resource in the summer season. Consequently, the proper management of aquifers and their stored energy is a new issue for public authorities, who require tools with which to forecast the evolution of groundwater temperatures.

The Water Framework Directive [14] and Directive 2015/1787/EC [15] are the most important laws in the European Union concerning water protection. The first aims to protect and improve the quality of water resources across Europe and sets environmental objectives for all water bodies, including groundwater. It requires member states to use their river basin management plans and programmes of measures to protect and, where necessary, restore the quality and quantity of water bodies in order to reach or maintain a good status. Directive 2015/1787/EC foresees the water quality control strategies according to the Water Safety Plan (WSP), introduced in 2004 by the World Health Organization [16], in order to determine the safety of water for human consumption. The main objective of the WSP is to ensure human health protection based on a careful risk analysis process that considers the entire water supply chain and the integrity of all the pumping well assets to ensure water quality and quantity for future generations.

The implementation of a proper WSP can minimize the risks and threats affecting the water system [17,18]. Recently, Muoio et al. [19] in the WSP of Tuscany (Italy) proposed a method for assessing water risk, whereas Van den Berg et al. [20] implemented a WSP in the Netherlands to evaluate different water management methods. Previous studies on WSP have demonstrated that improving the understanding of the system can contribute to more effective risk management as it reduces uncertainty in decision-making and increases the reliability of the system [21]. As claimed by F. La Vigna [22] for groundwater-resilient cities, a good understanding of both the hydrogeological system and groundwater flow processes are included in the general best practices, which are valid in all city types and hydrogeological contexts and allow for efficient water management based on a scientific interpretation of the observed phenomena. For these reasons, nowadays, numerical modeling plays a critical role in groundwater management by providing a framework for understanding complex hydrogeological processes [23], predicting future groundwater behavior, and evaluating the impacts of different management strategies [24]. Furthermore, simulating hydrogeological system behavior in response to potentially hazardous phenomena improves the ability of the water management system to respond to dangerous events [25] and enables decision-makers to optimize water use and protect groundwater resources [26]. Vazquez-Sunné et al. [27] published one of the first papers stating that urban groundwater was emerging as a distinct branch of hydrogeology and that numerical modeling was an essential tool for proper hydrogeological management. Most recently, Singh presented a comprehensive review on the numerical modeling applications for groundwater resources management [28]. In the literature, there are an increasing number of papers concerning the application of numerical modeling for groundwater management at the urban scale in cities like London [29], Lisbon [30], Berlin [31], Barcelona [32], Paris [33], Detroit [34], and New York City [35].

Among the types of groundwater models, steady-state models hold particular significance due to their focus on average conditions. By eliminating temporal fluctuations, these models offer a clear view of the basic aquifer's hydraulic properties, such as its transmissivity and hydraulic conductivity. Therefore, they are considered ideal for assessing aquifer characteristics and achieving a first parameters calibration, which is useful in implementing a more detailed unsteady-state model, ensuring an accurate initialization of dynamic simulations [26]. Steady-state models are inherently simpler to create, execute, and postprocess than unsteady-state models, and for that reason, when a modeling process starts, they are typically preferred, allowing for the easier achievement of a good calibration of the hydraulic parameters. Indeed, steady-state models are less suitable for making management forecasts involving strong temporal variations in boundary conditions, such as in the case of climate change, or high variations in the levels of large-surface water bodies [36]. However, they remain a cornerstone of hydrogeological analysis, providing

critical insights into aquifer behavior under average conditions, which is the cause of their still being widely applied in groundwater management.

The present study is part of a wider project named "MODEL-MI" founded by MM S.p.a., which is the manager of the water service for the public water supply in the city of Milan. The project's aim is to implement a groundwater flow model of Milan, which will be useful for the development of the WSP for the Milan FUA (Functional Urban Area), in collaboration with the service manager and other actors involved in the water management system (i.e., the ISS—Italian National Institute of Health; the ARPA—Lombardy Regional Agency for Environmental Protection; and the Municipality of Milan).

In this framework, the present paper deals with the definition of the hydrogeological conceptual model of the study area and the subsequent development of the steady-state groundwater flow model, which constitutes one of the tools for the WSP implementation and, in general, contributes to the proper management of the groundwater resource, predicting groundwater responses to environmental and anthropogenic pressures.

The main scientific contribution of this research lies in its demonstrating how a more detailed and robust stratigraphic characterization can improve the predictive capability of numerical models used for water resources management, even in well-known aquifers.

To this end, the present study addresses the following issues: (i) the reconstruction of a detailed hydrogeological conceptual model; (ii) the parametrization of the different aquifers; and (iii) the groundwater flow modeling implementation and calibration in steady-state conditions. The groundwater flow numerical model represents the starting point for subsequent studies on the implementation of an unsteady-state model and the simulation of future scenarios based on both socioeconomic changes (involving variation in pumping rate and recharge) and projections about global climate change that can influence future water availability and its quality. Some additional figures are reported in the Supplementary Materials from S1–S9.

2. Study Area

The study area is in the Lombardy Region and specifically falls in the Ticino-Adda groundwater basin (Figure 1), one of the most densely populated areas in the EU, where large urban areas (e.g., Milan Function Urban Area) coexist with extensive cultivation of crops alongside dairy farming and livestock rearing. This territory is bounded to the west by the Ticino River (average flow rate 350 m^3/s), which flows from the Lake Maggiore, and to the east by the Adda River (average flow rate 190 m^3/s), which flows from the Lake of Como. The hydrographic system also comprises three minor rivers, namely, Olona, Seveso, and Lambro, having an average flow rate in the Milan area of less than 10 m^3/s [37]. The area is also characterized by a dense canal network whose construction began in the 13th century and which still plays a crucial role in supplying irrigation water to the surrounding farmland. The six main irrigation waterways are the Villoresi, Martesana, Muzza, Naviglio Grande, Naviglio Bereguardo, and Naviglio Pavese (Figure 1). These canals, from April to September, diverge water from Ticino and Adda rivers, feeding agricultural fields (mainly flooding system) through a dense a gravity-driven irrigation network. The water needs of crops are almost entirely satisfied by river water, and groundwater has a minimal use for this purpose.

The climate is classified as temperate–continental, with cold winters and hot summers and a mean annual temperature of about 15 °C [38]. The mean annual precipitation of the last 20 years (2004-23) ranges from 717 mm in the southern part of the study area (Sant'Angelo L. station) to 1115 mm in the northern portion (Busto Arsizio station), with the highest precipitations in spring and autumn.

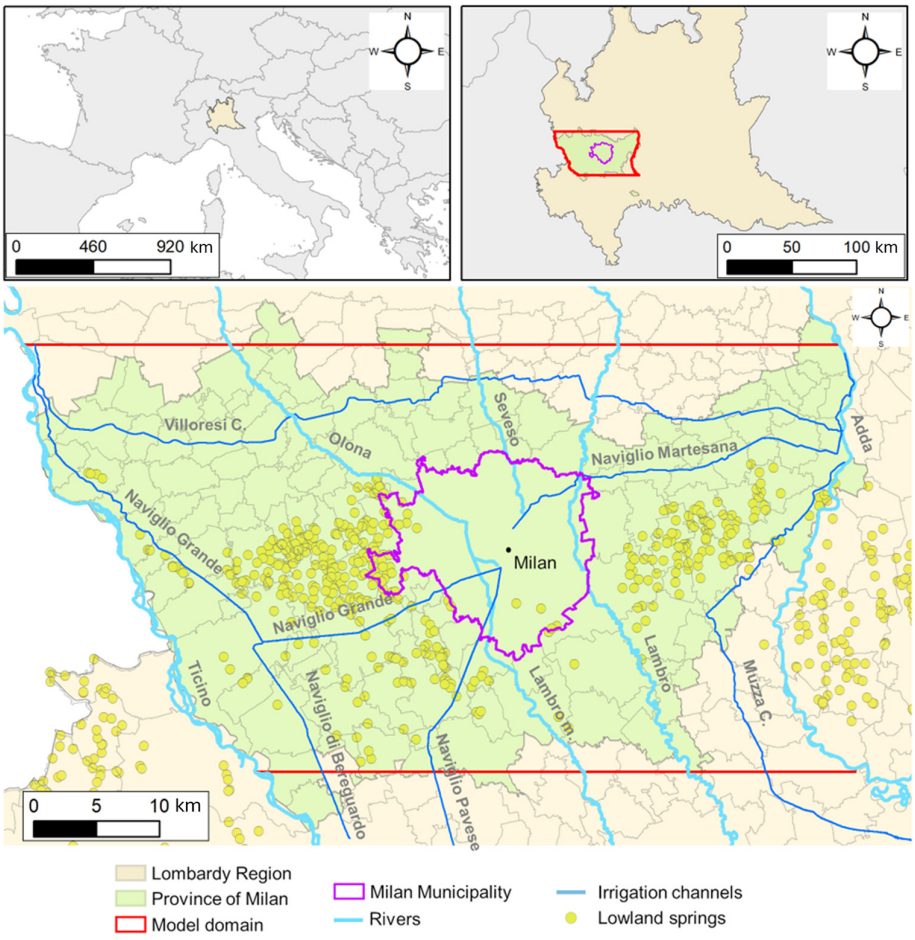

Figure 1. Location of the study area and extension of the model domain.

As the study mainly focuses on the urban area of Milan, the model domain was extended north and south, east and west, including almost the entire Province of Milan (Città Metropolitana di Milano), to set boundary conditions far enough from the area of interest. As explained in next section, the north and south boundaries do not correspond to physical boundaries, but their choice permitted us not to enlarge the domain extension too greatly and to use a finer discretization grid.

From a hydrogeological point of view, the area contains a wide regional aquifer, which extends from the Adda to the Ticino River, from the Prealps to the Po River, and is subdivided into eight GroundWater Bodies (GWB, as envisaged by Directive 2000/60/EC). The hydrogeological setting of the study area is well known, as in the past, it was subject to several investigations and previous studies, although these have often not been published in scientific journals [39,40].

In general, the aquifer-bearing alluvial deposits are a sequence of Plio-Pleistocenic sediments that filled the Po plain basin with a maximum thickness of about 500 m [41,42]. At the bottom of the sequence, the sediments are mainly clay and silt, whereas at the top, gravel and sand are predominant. Based on the glacial depositional cycles, these deposits can be divided into four hydrogeological units denoted as Aquifer Groups A, B, C, and D [43]. These units (from the youngest A to the oldest D) host aquifers which are separated by clayey deposits, acting as aquicludes at the regional scale. Only three of these Aquifer Groups have been extensively investigated through drillings in the Milan area [44,45]. In particular, the shallower Aquifer Groups A and B, which extend in the first 100–150 m of depth, are the most exploited ones, and these are the groups analyzed in this study. Aquifer Group A is mainly composed of gravels with sandy layers and represents the

shallow unconfined aquifer, with a base varying from 190 to 20 m a.s.l. It is characterized by high values of both hydraulic conductivity (ranging from 10^{-4} m/s to 10^{-3} m/s) and transmissivity (usually higher than 10^{-2} m^2/s). In the southern sector of the study area, Aquifer Group A is separated from the underlying Aquifer Group B by a clayey layer, which is not homogeneously distributed over the area of interest [46,47]. Aquifer Group B has a base varying from 140 to −100 m a.s.l., constitutes sands with silty–clayey lenses, has a hydraulic conductivity varying from 10^{-5} to 10^{-4} m/s, and a transmissivity ranging from 10^{-3} to 10^{-2} m^2/s. It consists of four different sub-units, called B1, B2, B3, and B4, which reflect the depositional cycles characterized by a grain size decreasing from the shallowest sub-unit (B1) to the deepest one (B4), with clayey layers ensuring their separation.

The groundwater flow is generally oriented north–south and is influenced by the main rivers, Ticino and Adda, mainly acting as gaining rivers [48]. At the transition zone between the high and low plain, a 20 km wide belt is characterized by the presence of lowland springs (i.e., fontanili) due to the decrease in grain size, passing from coarse sandy gravel to medium-fine sand, and the proximity of the water table to the topographic surface [49,50].

As the Po plain area, and more specifically Milan, depends on groundwater for industry and its public drinking supply, tools and measures for managing, preventing, and controlling groundwater quali/quantitative depletion are needed. Three main issues can be identified for the groundwater of Milan: quantity, quality, and temperature management.

As far as quantity is concerned, as a consequence of a water demand decrease in the industrial sector, since the 1970s, the city of Milan has experienced a significant rising trend with respect to the groundwater table, with relevant issues arising in the 1990s concerning the underground structures and infrastructure [51–53], like many other urban areas all over the world [54].

As far as water quality is concerned, in the area belonging to the Milan city, both point sources and diffuse contamination can affect groundwater, and they have been the subject of many previous studies [55]. Furthermore, in the last 20 years, Milano has experienced continuous growth in the number of GroundWater Heat Pumps systems (GWHP) for buildings conditioning, a technology that is expanding all over the world and mainly in highly urbanized areas because of the energy crisis [56–62]. The flow and solute or heat transport numerical models are useful tools not only in managing groundwater availability but also in assessing the effect of other features on groundwater quality, such as the effect of thermal perturbation due to geothermal systems or solute concentration variation due to pollution. To study these problems in detail, specific numerical models with specific experimental data need to be developed.

3. Materials and Methods

3.1. Hydrogeological Conceptual Model Implementation and Grid Discretization

The model was implemented using the Modflow-2005 code [63] (Ground Water Vistas interface, ESI Inc., Montgomeryville, PA, USA), a widely-used modular finite-difference groundwater flow model developed by the U.S. Geological Survey (USGS, Reston, VA, USA) designed for simulating and predicting groundwater flow dynamics in a variety of hydrogeologic settings [64]. The study area (approximately 1900 km^2) was discretized into a regular model grid of 338 rows and 663 columns with a cell resolution of 100 m. The detailed hydrogeological characterization of the Milan FUA subsoil required a comprehensive database, which was developed by collecting the existing databases provided by both public agencies and private companies. This database includes over 2750 well stratigraphies, encompassing information on location, screens position, lithological description, and layer depths (for a total number of about 40,000 stratigraphic layers). Together with the log-stratigraphic data, the construction and interpretation of hydrogeological sections

led to the defining of the thickness of both Aquifer Groups and the aquitards/aquicludes separating them. For this purpose, 16 cross-sections (Figure S1 in Supplementary Materials) were prepared at the basin scale (8 E-W and 8 N-S, on average 3.5 km spaced) in order to analyze the depositional trends and delineate the transition between the different Aquifer Groups (4 of them are reported in Supplementary Materials as S2, S3, S4, S5). Additionally, 66 local-scale cross-sections with variable orientation were generated for a detailed hydrogeological analysis near the pumping stations located within the Milan Municipality, as this was one of the main aims of the MODEL-MI project.

All the information on the bounding surfaces identified between the Aquifer Groups was imported into geological Modeling software, enabling the construction and visualization of the hydrogeological conceptual model through 3D interpolation. More specifically, the spatial interpolation was performed using the ordinary kriging method with linear trend removal and a specific smoothing factor. First, the surface of maximum hierarchical order, corresponding to the bottoms of Aquifer Groups A and B, was spatially interpolated. Subsequently, 3 surfaces of lower hierarchical order were reconstructed within Aquifer Group B, reflecting the hydrostratigraphic boundaries of 4 distinct sub-units (i.e., B1, B2, B3, B4). Each sub-unit is characterized by a fining upward sequence, within which a higher permeable layer, at the bottom, and a lower permeable layer, at the top, have been identified (Table 1 and Figure 2).

Table 1. Scheme representing the hydrogeological conceptual model.

Aquifer Groups	Aquifer Sub-Units	Permeability	Model Layer
A	A unconfined aquifer	High	1
	A/B separation	Low	2
B	B1 semiconfined aquifer	High	3
	B1/B2 separation	Low	4
	B2 confined aquifer	High	5
	B2/B3 separation	Low	6
	B3 + B4 confined aquifer	High	7

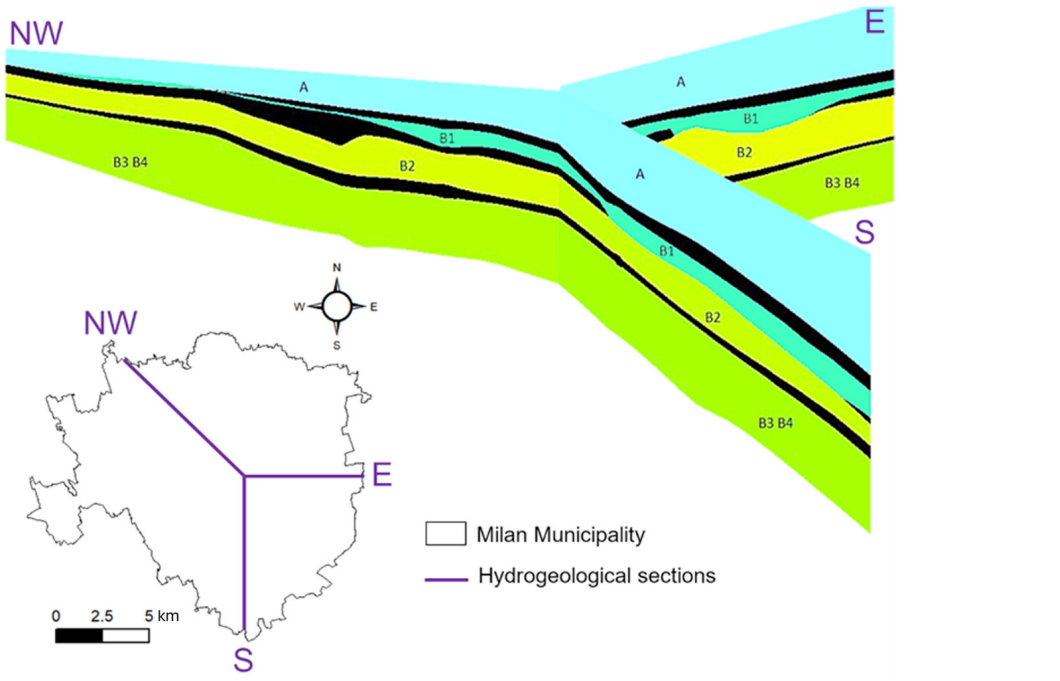

Figure 2. *Cont.*

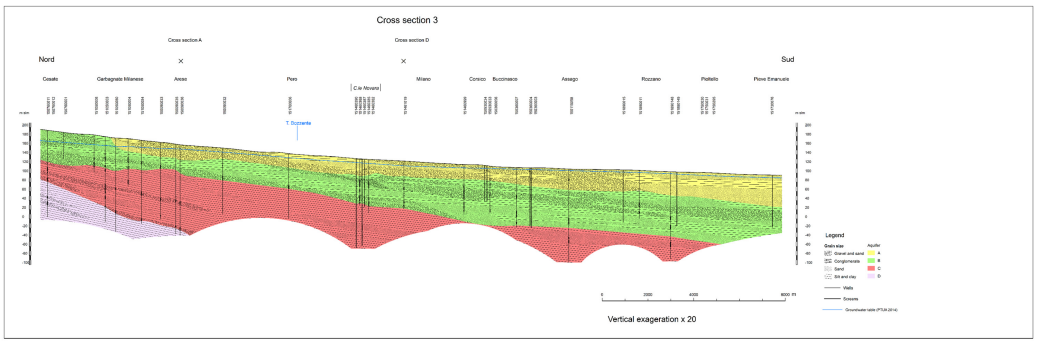

Figure 2. Example of hydrogeological cross-section of the study area (see also Figures S2–S5 in the Supplementary Materials). The letters A, B1, etc. refer to the aquifer sub-units described in Table 1.

The conceptual model comprises 7 distinct layers from the top to the bottom (Table 1 and Figure 2). Layer 1 represents Aquifer Group A, which extends from the land surface to a depth ranging from 190 to 20 m a.s.l., proceeding from NNW to SSE (Figure S6 in Supplementary). Aquifer Group A and the underlying Aquifer Group B are hydraulically separated by a low permeability level, which corresponds to layer 2. Stratigraphic well data reveal that this aquitard is not uniformly distributed throughout the study area. It is completely absent in the northeastern sector, where Aquifer Group A and sub-unit B1 are hydraulically interconnected, forming a single unconfined aquifer (Figures 2 and S8). Moving southward, the aquitard is first detected at the border with the Milan Municipality and gradually thickens (up to 10–12 m), leading Aquifer Group B to be more and more confined. As described above, Aquifer Group B was divided into 4 hydrogeological sub-units, identified as B1, B2, B3, and B4 (from top to bottom). The sub-unit B1, corresponding to layer 3, reaches its maximum thickness (15–20 m) in the southern sector of the study area, while in the northern sector, it is completely absent or is characterized by a very reduced thickness. The underlying sub-unit B2 consists of a low permeability level (layer 4) and a permeable level (layer 5). The low permeability level constitutes the top of sub-unit B2 and has a fairly constant thickness, varying between 5 and 10 m. Instead, the permeable level represents the aquifer of sub-unit B2 and has an average thickness, ranging from 15 to 25 m. Sub-units B3 and B4 are combined into a single layer (number 7) and are confined by a low permeability level (layer 6). This simplification was made due to limited data availability for these deep sub-units and the frequent presence of well screens in both. The sub-unit including both B3 and B4 is 5–10 m thick in the northern sector, whereas moving southward, its thickness increases, ranging between 20 and 30 m. Both the clayey layers at the top of sub-units B2 and B3–B4 (i.e., layers 4 and 6, respectively) are not uniformly distributed within the study area, especially in some portions of the northern sector where sub-units B1 and B2 and sub-units B2 and B3–B4 are hydraulically interconnected.

3.2. Piezometric Data and Hydraulic Conductivity

In the Milan area, after the strong rises in piezometric levels observed between 1970 and the end of the 1990s, a stabilization of hydraulic heads has been observed. These vary seasonally by some meters but generally, no trends have been observed in last 20 years. The piezometric morphology has assumed a stable form, as attested by the piezometric maps periodically produced by the Metropolitan City of Milan [65]. For this reason, in the first step of our work, it was decided to implement a model in steady-state conditions.

The ARPA (Regional Environmental Protection Agency), in 2014, established a piezometric monitoring network for Aquifer Groups A and B. At present, a specific monitoring network for each sub-unit identified within Aquifer Group B is not available. In

May 2014, the ARPA measured the groundwater level in 248 monitoring wells in the domain area, generating the piezometric maps of both the shallow unconfined aquifer (i.e., Aquifer Group A, Figure 3) and the underlying deeper aquifer (i.e., Aquifer Group B, in Figure S9 of Supplementary Materials). These piezometric maps are the most complete maps currently available for the study area, and they were used for both the boundary conditions and the model calibration process. Based on the hydrogeological conceptual model previously described and the screen depths of the available monitoring wells, 182 piezometric data were attributed to Aquifer Group A, and the remaining 66 were assigned to Aquifer Group B. In both aquifer groups groundwater flow is generally oriented NW–SE, with the water table decreasing from 190 to 70 m a.s.l. and an average hydraulic gradient of 2.5‰.

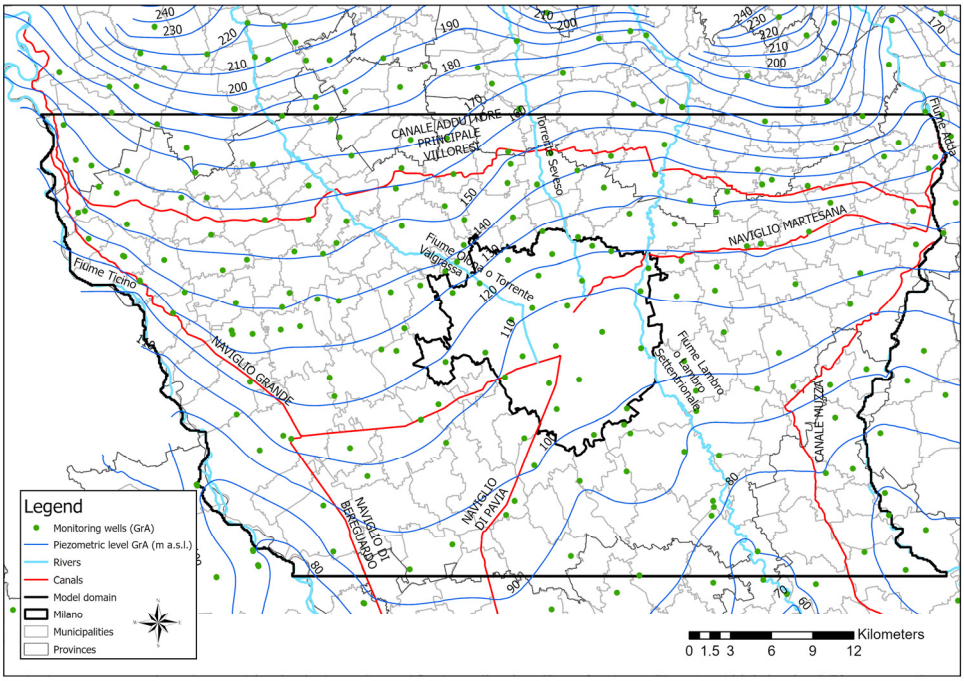

Figure 3. Piezometric map of Aquifer Group A generated using the piezometric data measured during the hydraulic head survey of May 2014 (the map for the deeper aquifer is shown in Figure S9).

The hydraulic conductivity values were initially assigned to each layer of the conceptual model considering the results derived from both the calibration of flow models implemented in previous studies [39] and the pumping tests available within the study area. A hydraulic conductivity value equal to 10^{-9} m/s was assigned to clay lenses within the different aquifer groups or sub-units after a calibration process where a value of 10^{-10} and 10^{-8} m/s was assigned to clay, and no difference in terms of hydraulic heads was achieved (i.e., layers 2, 4, and 6).

3.3. Boundary Conditions

Based on the piezometric maps described above, boundary conditions were applied to the model. Along the W and E borders of the model domain, the Ticino and Adda rivers were represented through Dirichlet boundary conditions (i.e., constant head) by assigning the average hydrometric levels measured along them in May 2014 (light blue lines in Table 2 and Figure 4). The Dirichlet condition refers to the assigning of a fixed (constant or specified) value of the hydraulic, and this value will not change during the numerical simulation; furthermore, the cell (where the BC is present) is deactivated and the value of the hydraulic head into cell is the specified one. The two rivers exhibit a relatively constant regime due to the flow rates regulation by dams and limited fluctuations in hydrometric

levels, typically lasting a few days. In a context characterized by rivers generally located in deeply engraved valleys, whose level is always lower than the groundwater level, even by several meters, the slight fluctuations of rivers have a minimal impact on groundwater piezometry morphology. Furthermore, considering the official piezometric maps elaborated by Provincia di Milano and Regione Lombardia over the past 30 years, the groundwater–river exchanges does not change over time and seasons. Therefore, within the model domain, the two rivers represent a physical boundary for Aquifer Group A, generally draining the groundwater system.

Table 2. Hydrometric stations with the hydrometric levels measured in May 2014 (corresponding to the stage assigned in the RIVER package).

Hydrometric Station	River	Water Level (m a.s.l.)
Cantù Asnago	Seveso	246.06
Castellanza C.so G. Matteotti	Olona	200.99
Golasecca Miorina misuratore	Ticino	189.92
Lesmo Peregallo	Lambro	177.39
Locate di Triulzi v. Staffora	Lambro m.	88.94
Lodi v. X Maggio	Adda	64.89
Milano v. Feltre	Lambro	115.24
Olginate S. Maria Lavello	Adda	193.25
Paderno Dugnano Palazzolo	Seveso	166.90
Pavia SS35	Ticino	57.53
Pizzighettone ponte Trento e Trieste	Adda	40.50
Rivolta d'Adda SP4	Adda	98.06
Salerano sul Lambro SP115	Lambro	60.70
Vigevano SS494	Ticino	57.53

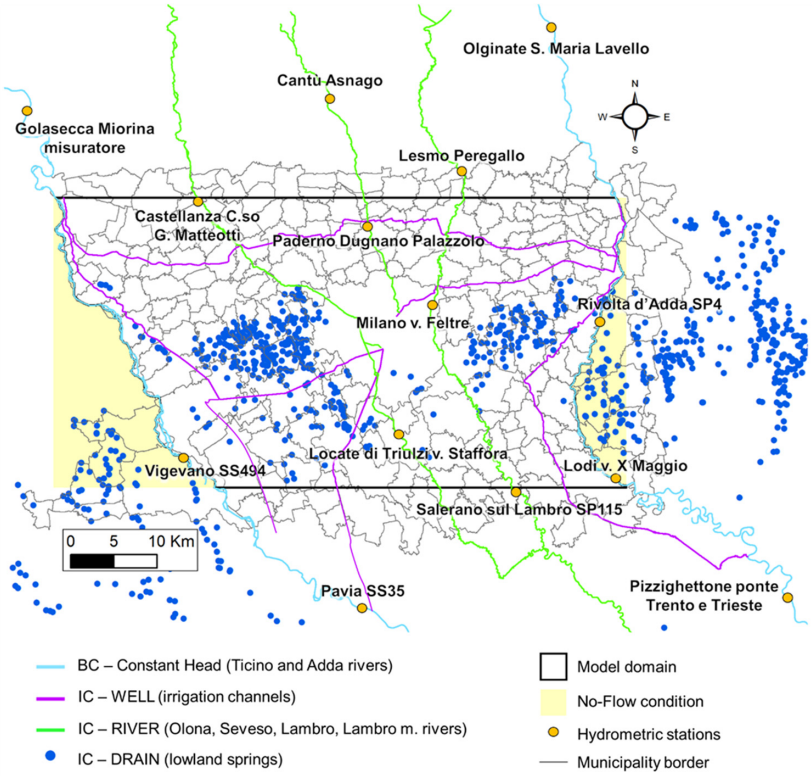

Figure 4. Map representing the Boundary Conditions (BC) and the Internal Conditions (IC) assigned to rivers, irrigation channels, and lowland springs within the model domain.

Constant heads (CH) were also applied along the northern and southern borders of the study area, with piezometric levels ranging from 190 to 135 m a.s.l. (from W to E)

along the northern border, and from 95 to 68 m a.s.l. (from W to E) along the southern one (light blue lines in Table 2 and Figure 4). Finally, the no-flow condition was assigned to cells located outside the model domain (yellow sectors in Figure 4). A CH condition was initially implemented for the northern and southern boundaries of the model, representing a hydraulic boundary. While there were no physical limits capable of controlling the groundwater level (as in the case of Adda and Ticino), a CH condition was chosen for this steady-state modeling phase due to the significant distance from the northern and southern limits from the area of primary interest (the city of Milan). This distance is large enough to prevent relevant influences on the model results in the area of interest. The head values were set based on the May 2014 piezometry, which extends beyond the domain and is free from boundary defects.

3.4. Internal Conditions: Rivers, Irrigation Canals, Lowland Springs and Wells

Within the modeling domain, the following internal conditions were applied:

- RIVERS: The Olona, Lambro, and Seveso rivers, using the Modflow RIVER package (green lines in Figure 4), were represented through a Cauchy boundary condition: a head-dependent flux condition which, in the RIVER option, calculates the water exchange between surface water bodies and aquifers considering the river bed characteristics. The hydrometric levels were assigned based on the interpolation of the daily average hydrometric levels measured in May 2014 (Table 2). Information with which to estimate the conductance and assess the groundwater interaction with these three rivers was gathered at Regione Lombardia (Geoportale della Regione Lombardia—www.geoportale.regione.lombardia.it (accessed on 30 October 2020).
- IRRIGATION CANALS: As well as the rivers, the study area features a dense network of irrigation canals which act as groundwater recharge zones. For the six main canals, information on water losses along their path is available from the land irrigation consortia. These channels were simulated using the Neumann boundary condition: a specified flux condition which allows use to set a flow rate entering or exiting from a specified model cell. The water supply via minor canals and irrigation activities on the fields was accounted for through the recharge, as explained in the next paragraph.
- LOWLAND SPRINGS: These springs, known as "fontanili", which are mainly located in the southern sector of the model domain, were represented trough a Cauchy boundary conditions using the Modflow DRAIN package (blue dots in Figure 4). This condition allowed us to simulate zones of groundwater emergence when the hydraulic head is higher than the land surface. Data on their location, elevation, and, in some cases, the estimated flow rate were derived from unpublished documents of Metropolitan City of Milan.
- WELLS: A total number of 3037 wells with their average withdrawals in 2014 were imported into the numerical model and assigned to specific layers based on their screen depths. Data were derived from different databases: (a) public databases SIF (Sistema Informativo Falda—Groundwater Information System) and CUI (Catasto Utenze Idriche—Inventory of Water Utilities) provided by Città Matropolitana di Milano and Regione Lombardia, respectively; and (b) private databases provided by water service companies MM S.p.a., CAP Holding S.p.a., and BrianzAcque s.r.l. The total average pumping rate in 2014 was 20.41 m^3/s, with approximately 60% extracted from public wells and the remaining from private wells.

3.5. Recharge

In the study area, the groundwater recharge is significantly influenced by the rainfall, irrigation practices, and water network losses within the urban areas. To account for these

factors, different recharge conditions were attributed based on the land cover inventory provided by the Agency of Services and Forest [66] of the Lombardy Region (Figure 5).

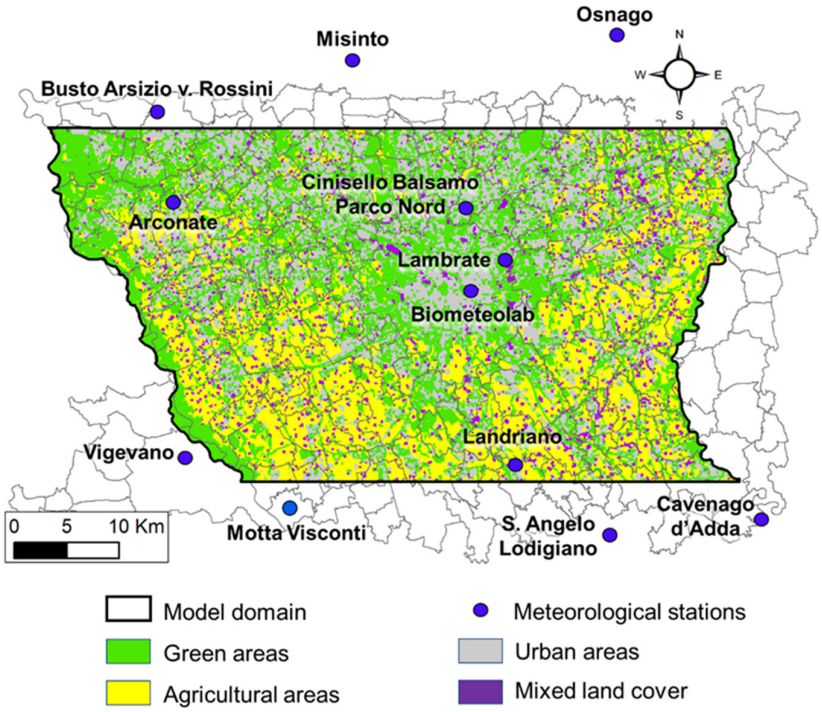

Figure 5. Map showing the land cover classification used to compute groundwater recharge.

Within the green and agricultural areas, the infiltration rate was quantified using the precipitation and temperature data (referring to the period January–August 2014) derived from 10 weather stations managed by the ARPA and from the meteorological station "Biometeolab" of the University of Milan. All available data were then processed with the Thornthwaite method [67] to determine the net precipitation after the evapotranspiration process. The resulting values were reduced by 30% to consider the surface run-off. The recharge value adopted for the steady-state model was chosen to be equal to the average of the values calculated for the period February–May 2014, corresponding to the months coinciding with and immediately preceding the reference piezometric campaign of May 2014.

The average recharge rate (Table 3) was estimated for the period February–May 2014, considering different soil uses. For the first category, the sole meteoric contribution was considered. In the agricultural areas, the contribution of irrigation was added to the meteoric recharge (considering the distributed irrigation volumes in spring 2014, provided by Consorzio Est Ticino Villoresi). Finally, for the urbanized areas, the recharge was estimated considering the water network leakages provided by MM (a value of 15% of the distributed water was considered).

Table 3. Recharge values range for the different soil use class.

Soil Use Class	Recharge Values Range (m/s)
Green areas	$9.5 \cdot 10^{-9}$–$1.3 \cdot 10^{-8}$
Agricultural areas	$9.5 \cdot 10^{-9}$–$1.6 \cdot 10^{-8}$
Urbanized areas	$2.0 \cdot 10^{-11}$–$9.3 \cdot 10^{-9}$

4. Model Calibration

The steady-state calibration process involved the estimation of the hydraulic conductivity in each model layer using the PEST parameter-estimation software (version 2010) [68,69]. This

software employs a set of points (i.e., "pilot points") distributed throughout the model domain to parameterize the spatial definition of the hydraulic property values. The pilot-point-based calibration initially consists of defining an interpolation method to obtain the distribution of parameter values over the entire model domain based on parameter measurements and the values at the pilot point locations. The spatial interpolation of the parameter values between pilot points is commonly performed using the kriging method. Then, the calibration process adjusts and optimizes the hydraulic property values to minimize the misfit between the computed and observed data, expressed by an objective function [70].

In this study, a regular grid with a 4 km spacing between pilot points was generated and subsequently increased by adding additional pilot points in areas where field observations were available (e.g., 99 pumping and slug tests) or where local calibrated flow models were already implemented and calibrated in previous studies. Given the large amount of available information, the calibration process was set up in such a way that the initial value attributed to each pilot point represented a preferred condition [70]. Moreover, specific ranges of variation were assigned to pilot points:

- A variability of ¼ of an order of magnitude above and below the initial value for pilot points reflecting field measurements.
- A variability of ½ of an order of magnitude above and below the initial value for pilot points located in areas where the K-field had already been calibrated.
- A variability of 1 order of magnitude above and below the initial value for the remaining pilot points.

A total number of 607 pilot points were added to the model and distributed within the different layers (including the low-permeability layers) belonging to the Aquifer Groups, as shown in Table 4 and in Figure 6.

Table 4. Subdivision of pilot points (PPs) in the different hydrogeological units and layers.

Hydrogeological Unit	Layer	# PPs
Aquifer A	1	225
Separation Aquifer A–Aquifer B	2	72
Semi-confining layers	3-4-6	79
Aquifer B	7	231

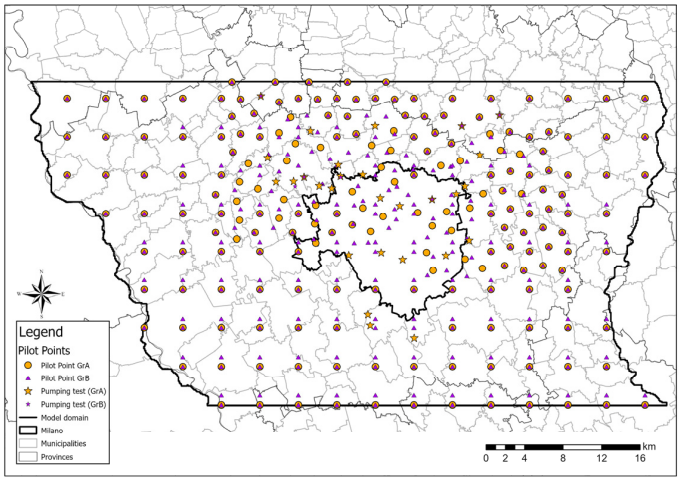

Figure 6. Map showing the distribution of the pilot points used to calibrate the hydraulic conductivity in each Aquifer Group.

The calibration targets were 248 piezometric level data measured in monitoring wells during the hydraulic head survey of May 2014.

5. Results and Discussion

5.1. Calibration Results

For each Aquifer Group and aquitard, the parameter-estimation process performed with PEST led to the definition of a calibrated K-field that properly reproduces field observations (Figure 7a,b). Using the kriging method based on an exponential model of the variogram, the hydraulic conductivity values were automatically assigned to each model cell through spatial interpolation from the pilot points to the entire model domain.

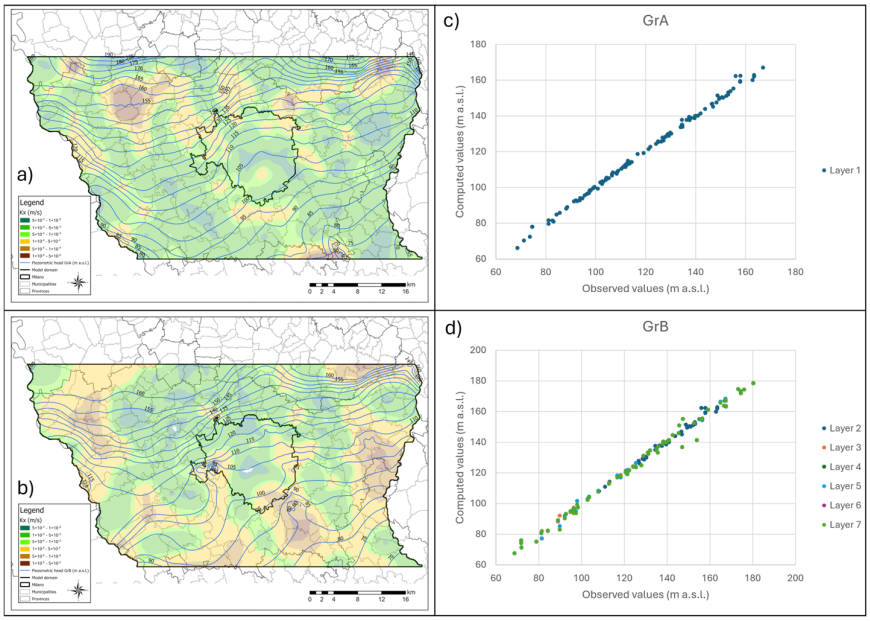

Figure 7. Maps (**a**,**b**) represent the distribution of the calibrated K-field and the computed piezometric head contours within Aquifer Groups A and B, respectively. The scatter plots show the degree of correlation between the observed and the simulated piezometric heads in Aquifer Group A (**c**) and in Aquifer Group B (**d**).

As reported in Table 5, the quality of the calibration results was evaluated by computing some statistical parameters. The residual mean and the absolute residual, which reflect the model-to-measurement misfit, provided a value equal to 0.18 m and 1.59 m, respectively, indicating a good fit between head measured and simulated heads. This is also evident in the plots of observed versus computed head target values. As shown in Figure 7c,d, the points fall on a straight line that has a slope of roughly 45 degrees, demonstrating the good agreement between observed and simulated heads in both Aquifer Groups A and B.

Table 5. Calibration statistics derived from the calibration of hydraulic conductivity.

Statistic	Calibration	Validation
Residual mean (m)	0.18	−1.09
Absolute residual mean (m)	1.59	1.99
Residual standard deviation (m)	2.59	2.22
Minimum residual (m)	−7.80	−7.46
Maximum residual (m)	12.70	4.79
Scaled absolute mean (%)	1.50	2.00
Scaled residual standard deviation (%)	2.30	2.30

The residual standard deviation and the absolute residual mean compared to the overall range of target values showed values below 10%, which is commonly assumed as a threshold for defining a calibration as good.

Subsequently, the model has undergone a validation process. The recharge and the well flow rates were updated to represent the conditions of February–May 2015, and the

observation dataset was updated using 498 water level measurements relative to April 2015. As shown in Table 5, the validation process confirms the goodness of the model under different conditions, with an absolute residual mean just slightly higher than the calibrated one and an even lower residual standard deviation.

The calibration results are showing an improvement compared the previous model calibrated for the Adda–Ticino Basin [48]. That model was implemented for a wider domain, including the urbanized area of Milan: the global absolute residual mean was 4.96 m, while in the Milano area, the error was reduced to 4.03 m, more than two times the absolute residual mean reported in Table 5. The calibration process represents an essential step to demonstrate the simulation capability of a numerical model and its reliability in simulating the behavior of the groundwater system. Sensitivity analysis and validation with a different dataset represent further important steps to improve the reliability of a model. These work steps are not presented here, but a sensitivity analysis was also conducted for both the hydrogeological parameters and the boundary conditions. Furthermore, a validation process was undertaken using data from the 2014–2018 period, but for reasons of length, it was not possible to present all the results in one manuscript, and they will be soon presented in a second paper. This represents the first limitation of the results presented in this article. The second limitation arises from the fact that it is a steady-state model that allows use to "take a picture" of a specific temporal instant (May 2014) and to calculate the mass balance for those specific boundary conditions (recharge, pumping rates, etc.). The model therefore provides important results, but their value can be extended only to periods that present conditions like those of our calibration period. Only through the implementation of an unsteady-state model that starts from the results of the steady-state one can we build a complete tool capable of calculating the water balance in different constraints and of forecasting the future behavior of the hydrogeological system. Finally, another limitation is the uncertainty concerning water withdrawn from private wells as this happens all over the world. While the public data are carefully collected, the private data often correspond to the volume granted by public authorities. Recently (2022), the Lombardy Region has implemented a new IT system (SIPIUI) that allows users to insert into a database the annual volumes extracted. This will undoubtedly allow us to improve the reliability of the model in the near future.

5.2. Water Budget

In this section, the mass balance resulting from the steady state simulation is analyzed. As reported in Table 6, the analysis was performed considering the contribution of the following:

- Recharge (Neuman condition);
- North and south boundary (Dirichelet condition);
- Main rivers (Dirichelet condition);
- Minor rivers (Cauchy condition);
- Leakages from the irrigation canals (Neumann condition);
- Lowland springs (Cauchy condition);
- Wells (Neuman condition).

Table 6. Contribution of each water budget component of the groundwater system.

Water Budget Component	Inflow	Outflow
RECHARGE (m^3/s)	31.10	-
CH (North and South) (m^3/s)	15.74	10.09
TICINO (m^3/s)	0.62	7.71
ADDA (m^3/s)	0.68	10.31
MINOR RIVERS (m^3/s)	1.91	5.68
WELLS (m^3/s)	-	20.41
CANALS (m^3/s)	4.10	-
SPRINGS (m^3/s)	-	0.21
TOTAL (m^3/s)	54.15	54.4
% error	−0.45	

The analysis of the water balance (Table 6) revealed an error, expressed as the difference between the water inflow and outflow, below 1%, which is commonly recognized to be the threshold value for considering the simulation results as good [26].

The water balance highlighted that the recharge (31.10 m^3/s) and the constant head boundary conditions (28.10 m^3/s), applied to the southern border and to the Adda and Ticino rivers, represent the largest water budget components and dominate the inflows and outflows of the system, accounting, respectively, for 57% and 52% of the total water budget. Groundwater withdrawal also has a marked effect on water balance, with a significant water outflow equal to 37.5%. The model confirms that the Adda and Ticino rivers are mainly draining the aquifer with 10.09 m^3/s and 7.71 m^3/s, respectively, the sum of which represents 33% of the total water budget, consistent with previous studies [48]. The minor rivers and lowland springs seem to have had the least impact on the system: Olona gives an inflow of 0.71 m^3/s and an outflow of 0.45 m^3/s, Lambro 1.06 m^3/s and 5.24 m^3/s, and Seveso is only feeding the groundwater with 0.15 m^3/s. The estimated drainage value for the Lambro is particularly interesting because it confirms a finding from a previous study [36]: Lambro has a significant drainage effect in the southern part of the domain, with an inflow comparable to its average flow rate. The simulated flow rates of lowland springs are very small and vary during the year, reaching the maximum value in the irrigation season and the minimum one in winter, when many of them become dry. As the simulation was conducted in a steady state in May, at the beginning of the irrigation activities, a low flow rate condition was certainly simulated. However, based on the authors' experience, the flow rate is largely underestimated. The reason for this model inaccuracy is linked to the limited information available for these springs. Nevertheless, the model balance could be little influenced by the lowland springs because the water that emerges from them is used in the irrigated fields located just downstream, mostly returning to the aquifer. Undoubtedly, the issue of lowland springs deserves further investigation, and the ongoing MAURICE project (EU Interreg Central) has among its aims a better understanding of their role in the groundwater balance and irrigation practices [3].

Finally, the model allowed us to evaluate the amount of water exchange between Aquifer Groups A and B thanks to the HSU package of Modflow. Aquifer Group A yields 15.1 m^3/s to Aquifer Group B, an exchange that occurs mainly north of Milan, where there is no hydraulic separation between the two systems. This exchange is relevant for Aquifer Group B considering that from the northern boundary, it is receiving an inflow of 9 m^3/s, and the withdrawal is 13.3 m^3/s.

6. Conclusions

The significant pressure that land transformation, population growth, rapid urbanization, and climate change impacts exert on water resources is becoming an important environmental issue in many densely urbanized areas, such as the Milan FUA. Under-

standing the hydrogeological system and its responses to these anthropogenic and natural stresses is crucial for achieving and ensuring a sustainable management of groundwater, especially for future generations, as well as for defining a reference groundwater level for urban planning and civil works design [71].

In this study, the implementation of a steady-state groundwater flow model provided a comprehensive and advanced tool with which to study groundwater system dynamics and understand the flow patterns at a regional scale. The considerable amount of stratigraphic data provided by both public and private companies led to a huge improvement in the construction of the regional hydrogeological conceptual model, allowing us to better represent the clay lenses and the separation of Aquifer Groups A and B, which constitute a unique aquifer in the northern sector while become separated in the southern one [46,72,73].

The results from both the calibration of the K-field within the different Aquifer Groups—results also supported by the validation procedure—and the mass balance highlighted that the improved numerical model can better reproduce the groundwater flow in a steady state at the regional scale. With the aim of exploring the effects of the expected climate change scenarios, the present numerical model has been used as a starting point for the implementation of a large-scale unsteady-state-conditions groundwater flow model that, once calibrated, will be used as a predictive tool for simulating the changes in water budget components and groundwater levels. The regional groundwater flow model will play a key role in supporting the water managers in assessing the groundwater system's response to future conditions and stresses, as well as in optimizing groundwater management and protection strategies.

Supplementary Materials: The following supporting information can be downloaded at: https://www.mdpi.com/article/10.3390/w17020165/s1, Figure S1: Hydrogeological cross-section traces; Figure S2: North–south hydrogeological cross-sections 4; Figure S3: North–south hydrogeological cross-sections 6; Figure S4: East–west hydrogeological cross-sections A; Figure S5: East–west hydrogeological cross-sections D; Figure S6: Bottom elevation in m a.s.l. of Aquifer Group A; Figure S7: Bottom elevation in m a.s.l. of the Aquifer Group B; Figure S8: Areal extension and thickness of the aquitard separating Aquifer Group A from Aquifer Group B; Figure S9: Groundwater head interpolation of the deep aquifer referred to (May 2014).

Author Contributions: Conceptualization, M.C. and P.G.; methodology, L.A., P.G. and L.C.; validation, M.A. and P.M.; data curation, F.M.; writing—original draft preparation, L.C. and P.G.; writing—review and editing, L.A. and M.A.; visualization, M.C. and L.C.; supervision, L.A. and P.G. All authors have read and agreed to the published version of the manuscript.

Funding: This research was funded by MM S.p.a., grant number 42/2017 CIG-7188325970.

Data Availability Statement: Data available on request due to restrictions eg privacy or ethical.

Acknowledgments: Thanks to I. La Licata, A. Ortelli, and L. Pollicino for their contribution in the fulfilment of the MODEL-MI project, and to., Regione Lombardia, ARPA Lombardia, Consorzio di Bonifica Est Ticino Villoresi, and CAP Holding for making the hydrogeological data available.

Conflicts of Interest: The authors declare no conflicts of interest. F. Marelli, on behalf of MM S.p.A., was responsible for the MODEL-MI project, playing an important coordination role between the Politecnico di Milano and the institutions in the collection of all data useful for numerical modeling. He had no role in the analysis and interpretation of data.

References

1. IPCC. Climate Change 2023: Synthesis Report. In *Contribution of Working Groups I, II and III to the Sixth Assessment Report of the Intergovernmental Panel on Climate Change*; Lee, H., Romero, J., Eds.; Core Writing Team: Geneva, Switzerland, 2023.
2. Corti, M.; Francioni, M.; Abbate, A.; Papini, M.; Longoni, L. Analysis and Modelling of the September 2022 Flooding Event in the Misa Basin. *Ital. J. Eng. Geol. Environ.* **2024**, *1*, 69–76. [CrossRef]

3. Colombo, P.; Mazzon, P.; Alberti, L. Off-season irrigation as a climate adaptation strategy for future groundwater management in Northern Italy. *Adv. Geosci.* **2024**, *64*, 27–31. [CrossRef]
4. Alberti, L.; Antelmi, M.; Oberto, G.; La Licata, I.; Mazzon, P. Evaluation of Fresh Groundwater Lens Volume and Its Possible Use in Nauru Island. *Water* **2022**, *14*, 3201. [CrossRef]
5. Omar, P.J.; Gaur, S.; Dwivedi, S.B.; Dikshit, P.K.S. Development and Application of the Integrated GIS-MODFLOW Model. *Microorg. Sustain.* **2021**, *24*, 305–314. [CrossRef]
6. Colombo, L.; Alberti, L.; Mazzon, P.; Antelmi, M. Null-Space Monte Carlo Particle Backtracking to Identify Groundwater Tetrachloroethylene Sources. *Front. Environ. Sci.* **2020**, *8*, 142. [CrossRef]
7. Antelmi, M.; Mazzon, P.; Höhener, P.; Marchesi, M.; Alberti, L. Evaluation of mna in a chlorinated solvents-contaminated aquifer using reactive transport modeling coupled with isotopic fractionation analysis. *Water* **2021**, *13*, 2945. [CrossRef]
8. Antelmi, M.; Alberti, L.; Barbieri, S.; Panday, S. Simulation of thermal perturbation in groundwater caused by Borehole Heat Exchangers using an adapted CLN package of MODFLOW-USG. *J. Hydrol.* **2021**, *596*, 126106. [CrossRef]
9. Epting, J.; Händel, F.; Huggenberger, P. Thermal management of an unconsolidated shallow urban groundwater body. *Hydrol. Earth Syst. Sci.* **2013**, *17*, 1851–1869. [CrossRef]
10. Guimerà, J.; Ortuño, F.; Ruiz, E.; Delos, A.; Pérez-Paricio, A. Influence of Ground-source Heat Pumps on groundwater. In Proceedings of the European Geothermal Congress 2007, Unterhaching, Germany, 30 May–1 June 2007; pp. 1–8.
11. Hancock, P.J.; Hunt, R.J.; Boulton, A.J. Preface: Hydrogeoecology, the interdisciplinary study of groundwater dependent ecosystems. *Hydrogeol. J.* **2009**, *17*, 1–3. [CrossRef]
12. Worsa-Kozak, M.; Arsen, A. Groundwater Urban Heat Island in Wrocław, Poland. *Land* **2023**, *12*, 658. [CrossRef]
13. Menberg, K.; Bayer, P.; Zosseder, K.; Rumohr, S.; Blum, P. Subsurface urban heat islands in German cities. *Sci. Total Environ.* **2013**, *442*, 123–133. [CrossRef]
14. Eur-lex Directive 2000/60/EC of the European Parliament and of the Council of 23 October 2000 Establishing a Framework for Community Action in the Field of Water Policy. 2014. Available online: http://data.europa.eu/eli/dir/2000/60/oj (accessed on 29 December 2024).
15. European Union. Commission Directive (EU) 2015/1787 of 6 October 2015 Amending Annexes II and III to Council Directive 98/83/EC on the Quality of Water Intended for Human Consumption. DIRECTIVE 2015/1787/EU. 2015. Available online: http://data.europa.eu/eli/dir/2015/1787/oj (accessed on 26 December 2024).
16. World Health Organization (WHO). *Guidelines for Drinking Water Quality*; World Health Organization (WHO): Geneva, Switzerland, 2011; pp. 307–442.
17. Setty, K.E.; Kayser, G.L.; Bowling, M.; Enault, J.; Loret, J.F.; Serra, C.P.; Alonso, J.M.; Mateu, A.P.; Bartram, J. Water quality, compliance, and health outcomes among utilities implementing Water Safety Plans in France and Spain. *Int. J. Hyg. Environ. Health* **2017**, *220*, 513–530. [CrossRef] [PubMed]
18. Shafiei, S.; Khazaei, M.; Nabizadeh, R.; Fahiminia, M.; Leili, M.; Razmju, V.; Ansari, R.; Aghaei, M. Conducting a Water Safety Plan (WSP) Relied on WHO Recommendations for the Assessment of Qom Desalinated Water Supply System. *Avicenna J. Environ. Health Eng.* **2017**, *4*, 24–28. [CrossRef]
19. Muoio, R.; Caretti, C.; Rossi, L.; Santianni, D.; Lubello, C. Water safety plans and risk assessment: A novel procedure applied to treated water turbidity and gastrointestinal diseases. *Int. J. Hyg. Environ. Health* **2020**, *223*, 281–288. [CrossRef]
20. Van Den Berg, H.H.J.L.; Friederichs, L.; Versteegh, J.F.M.; Smeets, P.W.M.H.; de Roda Husman, A.M. How current risk assessment and risk management methods for drinking water in The Netherlands cover the WHO water safety plan approach. *Int. J. Hyg. Environ. Health* **2019**, *222*, 1030–1037. [CrossRef] [PubMed]
21. Merrett, H.C.; Chen, W.T.; Horng, J.J. A structural equation model of success in drinking water source protection programs. *Sustainability* **2020**, *12*, 1698. [CrossRef]
22. La Vigna, F. Review: Urban groundwater issues and resource management, and their roles in the resilience of cities. *Hydrogeol. J.* **2022**, *30*, 1657–1683. [CrossRef]
23. Velasco, V.; Gogu, R.; Vázquez-Suñè, E.; Garriga, A.; Ramos, E.; Riera, J.; Alcaraz, M. The use of GIS-based 3D geological tools to improve hydrogeological models of sedimentary media in an urban environment. *Environ. Earth Sci.* **2013**, *68*, 2145–2162. [CrossRef]
24. Lypp, B.; Birle, E.; Cudmani, R. Statistical analysis of groundwater levels for the determination of design groundwater levels. In Proceedings of the 17th European Conference on Soil Mechanics and Geotechnical Engineering, ECSMGE 2019, Reykjavik, Iceland, 1–6 September 2019. [CrossRef]
25. Winz, I.; Brierley, G.; Trowsdale, S. The use of system dynamics simulation in water resources management. *Water Resour. Manag.* **2009**, *23*, 1301–1323. [CrossRef]
26. Anderson, M.P.; Woessner, W.W.; Hunt, R.J. *Applied Groundwater Modeling*; Academic Press: Cambridge, MA, USA, 2015; ISBN 978-0-12-058103-0.

27. Vázquez-Suñé, E.; Sánchez-Vila, X.; Carrera, J. Introductory review of specific factors influencing urban groundwater, an emerging branch of hydrogeology, with reference to Barcelona, Spain. *Hydrogeol. J.* **2005**, *13*, 522–533. [CrossRef]
28. Singh, A. Groundwater resources management through the applications of simulation modeling: A review. *Sci. Total Environ.* **2014**, *499*, 414–423. [CrossRef] [PubMed]
29. Jones, M.A.; Hughes, A.G.; Jackson, C.R.; Van Wonderen, J.J. Groundwater resource modelling for public water supply management in London. *Geol. Soc. Spec. Publ.* **2012**, *364*, 99–111. [CrossRef]
30. Carneiro, J.; Carvalho, J.M. Groundwater modelling as an urban planning tool: Issues raised by a small-scale model. *Q. J. Eng. Geol. Hydrogeol.* **2010**, *43*, 157–170. [CrossRef]
31. Haacke, N.; Frick, M.; Scheck-Wenderoth, M.; Schneider, M.; Cacace, M. 3-D Simulations of Groundwater Utilization in an Urban Catchment of Berlin, Germany. *Adv. Geosci.* **2018**, *45*, 177–184. [CrossRef]
32. Vázquez-Suñé, E.; Sánchez-Vila, X.; Carrera, J.; Marizza, M.; Arandes, R. Rising groundwater levels in Barcelona: Evolution and effects on urban structures. In *Groundwater in the Urban Environment*; Brookfield: Amsterdam, The Netherland, 1997; pp. 267–271.
33. Thierry, P.; Prunier-Leparmentier, A.M.; Lembezat, C.; Vanoudheusden, E.; Vernoux, J.F. 3D geological modelling at urban scale and mapping of ground movement susceptibility from gypsum dissolution: The Paris example (France). *Eng. Geol.* **2009**, *105*, 51–64. [CrossRef]
34. Teimoori, S.; O'leary, B.F.; Miller, C.J. Modeling shallow urban groundwater at regional and local scales: A case study in detroit, mi. *Water* **2021**, *13*, 1515. [CrossRef]
35. Karamouz, M.; Mahmoodzadeh, D.; Oude Essink, G.H.P. A risk-based groundwater modeling framework in coastal aquifers: A case study on Long Island, New York, USA. *Hydrogeol. J.* **2020**, *28*, 2519–2541. [CrossRef]
36. Townley, L.R. The response of aquifers to periodic forcing. *Adv. Water Resour.* **1995**, *18*, 125–146. [CrossRef]
37. ARPA Lombardia SIDRO—Sistema Informativo Idrologico. Available online: https://idro.arpalombardia.it/it/map/sidro/ (accessed on 29 December 2024).
38. Ceriani, M.; Carelli, M. *Carta Delle Precipitazioni Medie, Massime E Minime Annue Del Territorio Alpino Della Regione Lombardia (registrate nel periodo 1891–1990)*; Ufficio Rischi Geologici della Regione Lombardia: Milano, Italy, 2000.
39. ARPA Lombardia. *Progetto Plumes Integrazione—Report Finale*; ARPA Lombardia: Milano, Italy, 2016.
40. Forcella, V.; Francani, V.; Gattinoni, P.; Scesi, L. A 3D model of the aquifer of milan (Northern Italy). *Surv. Geol. Min. Ecol. Manag.* **2014**, *2*, 3–10. [CrossRef]
41. Perego, R.; Bonomi, T.; Fumagalli, M.L.; Benastini, V.; Aghib, F.; Rotiroti, M.; Cavallin, A. 3D reconstruction of the multi-layer aquifer in a Po Plain area. *Rend. Online Soc. Geol. Ital.* **2014**, *30*, 41–44. [CrossRef]
42. Bini, A. Stratigraphy, chronology and paleogeography of Quaternary deposits of the area between the Ticino and Olona rivers (Italy-Switzerland). *Geol. Insubrica* **1997**, *2*, 21–46.
43. Regione Lombardia Interventi Normativi per L'attuazione della Programmazione Regionale e di Modifica e Integrazione di Disposizioni Legislative—Collegato Ordinamentale 2010. 2010. Available online: https://normelombardia.consiglio.regione.lombardia.it/normelombardia/Accessibile/main.aspx?view=showdoc&iddoc=lr002010020500007 (accessed on 29 December 2024).
44. Pedretti, D.; Fernàndez-Garcia, D.; Bolster, D.; Sanchez-Vila, X. On the formation of breakthrough curves tailing during convergent flow tracer tests in three-dimensional heterogeneous aquifers. *Water Resour. Res.* **2013**, *49*, 4157–4173. [CrossRef]
45. Alberti, L.; Colombo, L.; Francani, V. The groundwater flow velocity distribution in the urban areas: A case study. *Ital. J. Eng. Geol. Environ.* **2014**, *14*, 17–26. [CrossRef]
46. Gorla, M.; Simonetti, R.; Righetti, C. Basin-scale hydrogeological, geophysical, geochemical and isotopic characterization: An essential tool for building a decision support system for the sustainable management of alluvial aquifer systems within the provinces of Milan and Monza-Brianza. *Acque Sotter.—Ital. J. Groundw.* **2016**, *5*, 33–47. [CrossRef]
47. Alberti, L.; Cantone, M.; Colombo, L.; Licata, I. La Model calibration using the automatic parameter estimation procedure (PEST) of the North-eastern zone of the Milan Functional Urban Area (Italy). *Acque Sotter.—Ital. J. Groundw.* **2018**, *7*, 27–38. [CrossRef]
48. Alberti, L.; Cantone, M.; Colombo, L.; Lombi, S.; Piana, A. Numerical modeling of regional groundwater flow in the Adda-Ticino Basin: Advances and new results. *Rend. Online Soc. Geol. Ital.* **2016**, *41*, 10–13. [CrossRef]
49. Fumagalli, N.; Senes, G.; Ferrario, P.S.; Toccolini, A. A minimum indicator set for assessing fontanili (lowland springs) of the Lombardy Region in Italy. *Eur. Countrys.* **2017**, *9*, 1–16. [CrossRef]
50. De Luca, D.A.; Destefanis, E.; Forno, M.G.; Lasagna, M.; Masciocco, L. The genesis and the hydrogeological features of the Turin Po Plain fontanili, typical lowland springs in Northern Italy. *Bull. Eng. Geol. Environ.* **2014**, *73*, 409–427. [CrossRef]
51. Colombo, L.; Gattinoni, P.; Scesi, L. Stochastic modelling of groundwater flow for hazard assessment along the underground infrastructures in Milan (northern Italy). *Tunn. Undergr. Space Technol.* **2018**, *79*, 110–120. [CrossRef]
52. Gattinoni, P.; Scesi, L. The groundwater rise in the urban area of Milan (Italy) and its interactions with underground structures and infrastructures. *Tunn. Undergr. Space Technol.* **2017**, *62*, 103–114. [CrossRef]
53. Beretta, G.P.; Stevenazzi, S. Specific yield of aquifer evaluation by means of a new experimental algorithm and its applications. *Acque Sotter.—Ital. J. Groundw.* **2018**, *7*, 39–46. [CrossRef]

54. Frommen, T.; Moss, T. Pasts and presents of urban socio-hydrogeology: Groundwater levels in berlin, 1870–2020. *Water* **2021**, *13*, 2261. [CrossRef]
55. Alberti, L.; Colombo, L.; Formentin, G. Null-space Monte Carlo particle tracking to assess groundwater PCE (Tetrachloroethene) diffuse pollution in north-eastern Milan functional urban area. *Sci. Total Environ.* **2018**, *621*, 326–339. [CrossRef] [PubMed]
56. Antelmi, M.; Turrin, F.; Zille, A.; Fedrizzi, R. A New Type in TRNSYS 18 for Simulation of Borehole Heat Exchangers Affected by Different Groundwater Flow Velocities. *Energies* **2023**, *16*, 1288. [CrossRef]
57. Barbieri, S.; Antelmi, M.; Panday, S.; Baratto, M.; Angelotti, A.; Alberti, L. Innovative numerical procedure for simulating borehole heat exchangers operation and interpreting thermal response test through MODFLOW-USG code. *J. Hydrol.* **2022**, *614*, 128556. [CrossRef]
58. Chae, H.; Nagano, K.; Sakata, Y.; Katsura, T.; Kondo, T. Estimation of fast groundwater flow velocity from thermal response test results. *Energy Build.* **2020**, *206*, 109571. [CrossRef]
59. Piga, B.; Casasso, A.; Pace, F.; Godio, A.; Sethi, R. Thermal impact assessment of groundwater heat pumps (GWHPs): Rigorous vs. simplified models. *Energies* **2017**, *10*, 1385. [CrossRef]
60. Perego, R.; Dalla Santa, G.; Galgaro, A.; Pera, S. Intensive thermal exploitation from closed and open shallow geothermal systems at urban scale: Unmanaged conflicts and potential synergies. *Geothermics* **2022**, *103*, 102417. [CrossRef]
61. Bucci, A.; Prevot, A.B.; Buoso, S.; De Luca, D.A.; Lasagna, M.; Malandrino, M.; Maurino, V. Impacts of borehole heat exchangers (BHEs) on groundwater quality: The role of heat-carrier fluid and borehole grouting. *Environ. Earth Sci.* **2018**, *77*, 175. [CrossRef]
62. Berta, A.; Gizzi, M.; Taddia, G.; Lo Russo, S. The role of standards and regulations in the open-loop GWHPs development in Italy: The case study of the Lombardy and Piedmont regions. *Renew. Energy* **2024**, *223*, 120016. [CrossRef]
63. Harbaugh, A.W. MODFLOW-2005: The U.S. Geological Survey modular ground-water model—The ground-water flow process. Book 6: Modeling techniques, Section A. Ground-water. In *Techniques and Methods*; U.S. Geological Survey: Reston, VI, USA, 2005.
64. Musacchio, A.; Mas-Pla, J.; Soana, E.; Re, V.; Sacchi, E. Governance and groundwater modelling: Hints to boost the implementation of the EU Nitrate Directive. The Lombardy Plain case, N Italy. *Sci. Total Environ.* **2021**, *782*, 146800. [CrossRef] [PubMed]
65. Città Metropolitana di Milano Dati Acqua e Falda Provincia di Milano. Available online: https://www.cittametropolitana.mi.it/open_data/dataset-pubblicati-per-categoria/ambiente/dati_acqua_provincia.html (accessed on 30 October 2020).
66. ERSAF (Ente Regionale per I Servizi all'Agricoltura e alle Foreste) DUSAF (Destinazione d'Uso dei Suoli Agricoli e Forestali) [Land Use Database]. Available online: http://www.cartografia.regione.lombardia.it/ (accessed on 30 April 2018).
67. Thornthwaite, C.W.; Mather, J.R. The Water Balance. *Public Climatol.* **1955**, *8*, 5–86.
68. Doherty, J.; Hunt, R.J. Response to Comment on "Two statistics for evaluating parameter identifiability and error reduction". *J. Hydrol.* **2010**, *380*, 489–496. [CrossRef]
69. Doherty, J. *PEST, Model-Independent Parameter Estimation—User Manual*, 5th ed.; Watermark Numerical Computing: Brisbane, Australia, 2010.
70. Doherty, J. Ground water model calibration using pilot points and regularization. *Ground Water* **2003**, *41*, 170–177. [CrossRef]
71. Gattinoni, P.; Colombo, L.; Marelli, F.; Ortelli, A.; Scesi, L.; Alberti, L. Design Groundwater Level in Urban Areas Affected by Water Table Rising Trend: The Case Study of Milan. In Proceedings of the IAHR World Congress, Granada, Spain, 19–24 June 2022; pp. 1875–1882.
72. De Caro, M.; Crosta, G.; Frattini, P.; Castellanza, R.; Tradigo, F.; Mussi, A.; Cresci, P. Blue-green infrastructures and groundwater flow for future development of Milano (Italy). In Proceedings of the 17th European Conference on Soil Mechanics and Geotechnical Engineering, ECSMGE 2019, Reykjavik, Iceland, 1–6 September 2019. [CrossRef]
73. Giuliano, G. Ground water in the Po basin: Some problems relating to its use and protection. *Sci. Total Environ.* **1995**, *171*, 17–27. [CrossRef]